

# Ganglioside GM1 Deficiency in Effector T Cells From NOD Mice Induces Resistance to Regulatory T-Cell Suppression

Gusheng Wu,<sup>1</sup> Zi-Hua Lu,<sup>1</sup> Hans-Joachim Gabius,<sup>2</sup> Robert W. Ledeen,<sup>1</sup> and David Bleich<sup>3</sup>

**OBJECTIVE**—To detect GM1 deficiency and determine its role in effector T cells (Teffs) from NOD mice in establishing resistance to regulatory T-cell (Treg) suppression.

**RESEARCH DESIGN AND METHODS**—CD4<sup>+</sup> and CD8<sup>+</sup> Teffs were isolated from spleens of prediabetic NOD mice for comparison with similar cells from Balb/c, C57BL/6, and NOR mice. GM1 was quantified with thin-layer chromatography for total cellular GM1 and flow cytometry for cell-surface GM1. Suppression of Teff proliferation was determined by application of GM1 cross-linking agents or coculturing with Tregs. Calcium influx in Teffs was quantified using fura-2.

**RESULTS**—Resting and activated CD4<sup>+</sup> and CD8<sup>+</sup> Teffs of NOD mice contained significantly less GM1 than Teffs from the other three mouse strains tested. After activation, NOD Teffs resisted suppression by Tregs or GM1 cross-linking agents in contrast to robust suppression of Balb/c Teffs; this was reversed by preincubation of NOD Teffs with GM1. NOD Teffs also showed attenuated Ca<sup>2+</sup> influx via transient receptor potential channel 5 (TRPC5) channels induced by GM1 cross-linking, and this, too, was reversed by elevation of Teff GM1.

**CONCLUSIONS**—GM1 deficiency occurs in NOD Teffs and contributes importantly to failed suppression, which is rectified by increasing Teff GM1. Such elevation also reverses subthreshold Ca<sup>2+</sup> influx via TRPC5 channels, an essential aspect of suppression. Our results also support a critical role for galectin-1 as a GM1 cross-linking counter-receptor that fittingly is upregulated and released by Tregs during activation. These findings suggest a novel mechanism by which pathogenic Teffs evade regulatory suppression, thereby leading to autoimmune  $\beta$ -cell destruction and type 1 diabetes. *Diabetes* 60:2341–2349, 2011

**P**ancreatic  $\beta$ -cell destruction in type 1 diabetes is the net effect of antigen-specific effector T cells (Teffs) evading the protective defense of regulatory T cells (Tregs) (1,2). The homeostatic balance between Teffs and Tregs is critically important in maintaining control over “rogue” effector responses that lead to autoimmune disease (2). Studies in NOD mice have identified defects in both Teff and Treg populations that contribute to

immune islet damage. However, recent work has demonstrated that Tregs purified from NOD and Balb/c mice are capable of suppressing the proliferative response of Teffs obtained from Balb/c mice, but not from NOD mice (3). Similar findings have been demonstrated in human subjects with type 1 diabetes compared with nondiabetic control subjects and subjects with type 2 diabetes (4). These studies suggest that NOD mice and human subjects with type 1 diabetes both harbor a primary defect in Teffs that confers resistance to Treg suppression. This as yet biochemically undefined functional defect in Teffs is likely to play an important role in the pathogenesis of type 1 diabetes. This study was designed to test the hypothesis of deficient functional interplay between the protein effector, galectin-1 (Gal-1), and its ganglioside counter-receptor, GM1.

Ganglioside GM1 is an integral component of lipid raft microdomains with numerous functions, including regulation of Ca<sup>2+</sup> channel activity and coincident downstream signaling (5,6). Of particular note in this context is the robust upregulation of GM1 in Teffs during polyclonal activation that promotes more extensive cross-linking of cell-surface GM1 by homodimeric Gal-1, a protein secreted by Tregs; such interaction was previously shown to activate transient receptor potential channel 5 (TRPC5) Ca<sup>2+</sup> channels and suppress further Teff proliferation (7). This interaction between GM1 on Teffs and secreted Gal-1 from Tregs is one mechanism by which Tregs apparently can maintain homeostatic control over “rogue” Teff populations. The observation that the cholera toxin B (CtxB) subunit, a multivalent counter-receptor that binds with high affinity and specificity to GM1 (8), produced the same effects as the Treg product Gal-1 served to emphasize the pivotal role of GM1 cross-linking in Teff suppression (7). Thus, GM1 could function as a molecular switch in Teff homeostasis.

In the current study, we identify for the first time a fundamental deficiency of cell-surface GM1 in CD4<sup>+</sup> and CD8<sup>+</sup> Teffs from NOD mice that we propose underlies their resistance to Treg suppression. NOD Teffs are shown to resist TRPC5-mediated Ca<sup>2+</sup> influx and proliferation suppression when treated with Gal-1 or CtxB. Pretreatment of NOD Teffs with GM1 enhanced Ca<sup>2+</sup> influx and restored Teff suppression by both Tregs and the two previously mentioned GM1 cross-linking agents. Significantly, anti-Gal-1 antibody (Ab) blocked Balb/c Treg suppression of Teffs, pointing to Gal-1 as key effector in this form of intercellular communication. These results are consonant with NOD mouse studies in which type 1 diabetes was prevented by Gal-1 (9) and delayed with reduced frequency by GM1 (10). This action of Gal-1 parallels that previously reported for CtxB in preventing diabetes in the NOD mouse (11). Our findings suggest a novel mechanism by which pathogenic Teffs escape regulatory suppression, thereby leading to autoimmune  $\beta$ -cell destruction and type 1 diabetes.

From the <sup>1</sup>Department of Neurology and Neurosciences, New Jersey Medical School–University of Medicine and Dentistry of New Jersey, Newark, New Jersey; the <sup>2</sup>Institute of Physiological Chemistry, Faculty of Veterinary Medicine, Ludwig-Maximilians-University Munich, Munich, Germany; and the <sup>3</sup>Department of Medicine, New Jersey Medical School–University of Medicine and Dentistry of New Jersey, Newark, New Jersey.

Corresponding author: Robert W. Ledeen, ledeenro@umdnj.edu, or David Bleich, bleichda@umdnj.edu.

Received 20 September 2010 and accepted 4 June 2011.

DOI: 10.2337/db10-1309

R.W.L. and D.B. are cosenior authors.

© 2011 by the American Diabetes Association. Readers may use this article as long as the work is properly cited, the use is educational and not for profit, and the work is not altered. See <http://creativecommons.org/licenses/by-nc-nd/3.0/> for details.

## RESEARCH DESIGN AND METHODS

**Preparation and activation of Teffs and Tregs.** CD4<sup>+</sup> and CD8<sup>+</sup> Teffs were prepared from spleens of 8- and 11-week-old female Balb/c, NOD, NOR, and C57BL/6 mice (Jackson Laboratories, Bar Harbor, ME), as previously described (7). CD4<sup>+</sup> CD25<sup>+</sup> forkhead box transcription factor P3 (FoxP3<sup>+</sup>) Tregs were prepared from the spleens of Balb/c and NOD mice (7). The later cells were isolated with immunomagnetic bead kits (Miltenyi, Auburn, CA) according to manufacturer's instructions. CD4<sup>+</sup> T cells were first isolated by negative selection, followed by positive selection with anti-CD25-coated beads to yield Tregs. Purity of Tregs was verified with the Mouse Regulatory T Cell Staining Kit (eBioscience, San Diego, CA) and flow cytometry. In our hands, the CD4<sup>+</sup>CD25<sup>+</sup> T-cell population was ~90% positive for FoxP3<sup>+</sup>, as assessed by flow cytometry. Teffs were isolated by positive selection with anti-CD4- and anti-CD8-coated beads.

A portion of freshly isolated Teffs (resting cells) was used for lipid extraction and ganglioside analysis, and the remainder was activated by culturing 3 days ( $5 \times 10^5$  cells/mL) at 37°C in 5% CO<sub>2</sub> in the presence of anti-CD3/anti-CD28-containing Mouse T Cell Expander Dynabeads (Invitrogen, Carlsbad, CA). This was done in RPMI-1640 medium supplemented with 10% heat-inactivated FBS, penicillin (100 units/mL), streptomycin (100 µg/mL), L-glutamine (2 mmol/L), pyruvate (0.2 mmol/L), nonessential amino acids (0.5 mmol/L), HEPES (5 mmol/L), and β-mercaptoethanol (50 µmol/L). Treg cells were activated in the same medium with the addition of recombinant human interleukin-2 (10 ng/mL).

**Ganglioside analysis.** To visualize and quantify total cellular gangliosides, resting and activated CD4<sup>+</sup> and CD8<sup>+</sup> Teffs were extracted with chloroform/methanol (1:1 by vol). After brief centrifugation at 2,000g, the lipid extracts in the supernatant were removed from the protein pellets and applied to silica gel-coated high-performance thin-layer chromatography (HPTLC) plates (Fisher Scientific, Pittsburgh, PA) in volumes corresponding to equal protein amounts from each pellet. Varying amounts of bovine brain ganglioside mixture were applied to the same plate for quantification.

After development in chloroform/methanol/0.2 mol/L KCl (5:4:1 by vol), the plates were dried and treated sequentially with *Clostridium perfringens*-type V neuraminidase (N'ase; Sigma, St. Louis, MO), and CtxB conjugated to horseradish peroxidase (CtxB-HRP; Sigma), as described (12). Gangliosides were revealed on HyBlot CL Autoradiographic film (Denville, Metuchen, NJ) with Amersham ECL reagent and quantified by densitometry (Fluorchem Imaging, Alpha Innotech, San Leandro, CA) at sensitivities of 5–25 ng ganglioside sialic acid. Accuracy of detection was not subject to interference by the other cellular lipids, most of which migrated well ahead of gangliosides in the polar solvent system.

Cell surface GM1 and GD1a were determined by flow cytometry of viable Teffs, both resting and activated. The cells were incubated with 1 µg/mL CtxB-fluorescein isothiocyanate (FITC) for 30 min, or with anti-GD1a monoclonal Ab (mAb [1:800]; Chemicon, Temecula, CA) for 1 h, followed by goat anti-mouse IgG-FITC (1:200) for 1 h in PBS containing 2% BSA at 4°C. Cells were fixed with 0.5% paraformaldehyde and photographed with a Diaphot microscope (Nikon, Melville, NY) and analyzed with an LSR II air-cooled four-laser benchtop flow cytometer (BD Biosciences, San Jose, CA).

**Gal-1 and related reagents.** As described (7), human Gal-1 was isolated after recombinant production and its purity ascertained by one- and two-dimensional gel electrophoresis and mass spectrometry (13). To preclude gradual inactivation by oxidation, reactive thiol groups were protected by iodoacetamide treatment, ensuring maintained lectin activity with its binding to GM1 pentasaccharide (14). The Gal-1-specific Ab was raised in rabbits and rigorously checked for lack of cross-reactivity against other human galectins by Western blotting/enzyme-linked immunosorbent assay, excluding any respective reactivity by depletion using affinity chromatography on Gal-1-loaded resin (15). Gal-1 is highly homologous between species; human Gal-1 was shown to react in mouse systems and the above anti-Gal-1 Ab with mouse Gal-1 (16).

**Intracellular free Ca<sup>2+</sup> measurement.** As previously described (7), activated CD4<sup>+</sup> and CD8<sup>+</sup> T cells were treated with N'ase (0.5 units/mL) for 2 h at 37°C, then incubated with fura 2-acetoxymethyl (AM) ester (5 µmol/L) and sulfapyrazone (0.25 mmol/L) for 30 min. In some experiments, T cells were treated with mouse anti-GM1 IgG mAb (30 µg/mL; a gift of Dr. Kazim Sheikh, University of Texas Health Sciences Center, Houston, TX) or control mouse IgG in combination with fura 2-AM. In addition, aliquots of  $1-1.5 \times 10^5$  cells were suspended in buffered saline solution containing 20 mmol/L 4-morpholinepropanesulfonic acid (pH 7.2), 140 mmol/L NaCl, 5 mmol/L KCl, 1 mmol/L MgCl<sub>2</sub>, 10 mmol/L glucose, 0.25 mmol/L sulfapyrazone, 1% BSA, and 5 mmol/L CaCl<sub>2</sub>.

For inhibition studies, cells in suspension were preincubated 15–30 min with 100 µmol/L SK&F 96365, a TRP channel inhibitor. Measurements were performed with an RF-M 2001 fluorometer equipped with magnetic stirrer (Photon Technology, Monmouth Junction, NJ) for 700 s. CtxB (5 µg/mL) and Gal-1 (20 µg/mL) were applied at the times indicated. Fluorescence was induced by two excitation wavelengths at 340 and 380 nm, and one emission wavelength

at 510 nm was recorded. Intracellular calcium [Ca<sup>2+</sup>]<sub>i</sub> levels are expressed as the intensity ratio between the two excitation wavelengths (R<sub>340/380</sub>). Peak increases of [Ca<sup>2+</sup>]<sub>i</sub> after addition of CtxB or Gal-1 were compared.

**Teff proliferation assay.** Cell growth was assessed by tritiated thymidine [<sup>3</sup>H]TdR incorporation, as described (7). CD4<sup>+</sup> and CD8<sup>+</sup> Teffs from NOD and Balb/c mice, activated for 3 days as above, were transferred to 96-well flat-bottom plates ( $5 \times 10^4$  cells/100 µL/well) in the presence or absence of varying amounts of activated Tregs (see above) from the same or the counter strain. In some experiments, Teffs were preincubated with 100 µmol/L GM1 (gift from Fidia Research Laboratories, Abano Terme, Italy) dissolved in culture medium for 2 h. The cells were harvested 18 h after addition of 0.3 µCi [<sup>3</sup>H]TdR (American Radiolabeled Chemicals, St. Louis, MO) by filtration and radioactivity determined by liquid scintillation counting. Six wells were used for each experimental condition, and each experiment was repeated at least twice. In all cases, each assay had a set of wells that contained Tregs only (Teff/Treg = 0/1), which provided background counts that were subtracted in proportion to the number of Tregs in the mixture. Additional sets of wells contained mixed cultures with the indicated Teff/Treg ratios. Background counts were ~500 disintegrations per minute (DPM) per  $5 \times 10^4$  Tregs, which was ~17% of DPM in Teff-only cultures ( $5 \times 10^4$  cells) and less in cultures with Teff/Treg ratios between 1/0 and 1/1. For cultures with ratios between 1/1 and 1/4 the background subtractions were >500 DPM.

To assess the role of Gal-1, anti-Gal-1 Ab (10 µg/mL), which blocks binding to carbohydrate ligands, was added to wells containing Tregs and Teffs from the same strains. Similar assays were applied to Teffs treated with CtxB (0–20 µg/mL) or Gal-1 (0–100 µg/mL). In some experiments, anti-GM1 IgG Ab (non-cross-linking; 15 µg/mL) was applied to block the effect of these GM1 cross-linking reagents.

**Statistics and methods of analysis.** Ganglioside quantification was performed with 4–16 animals in each group, and [Ca<sup>2+</sup>]<sub>i</sub> measurements were repeated 3–4 times; the differences in both assays were analyzed by two-tailed Student *t* test. Each [<sup>3</sup>H]TdR incorporation experiment for cell proliferation was repeated at least three times, and one representative experiment was presented in which each treatment included six wells. Statistical differences were analyzed with one-way ANOVA with repeated measurements and the Tukey multiple comparison post-test. Calculations were made with Prism software (GraphPad, San Diego, CA).

## RESULTS

**GM1 and GD1a deficiency in NOD Teffs.** CD4<sup>+</sup> and CD8<sup>+</sup> Teffs from NOD, Balb/c, NOR, and C57BL/6 mice were activated with anti-CD3/CD28 or left untreated as resting (preactivated) cells. Extracted gangliosides from these cell populations were analyzed via HPTLC with N'ase/CtxB-HRP overlay, as described. Figure 1 indicates cellular ganglioside patterns for 8-week-old mice, revealing significant deficiencies of GM1 and GD1a in Teffs from NOD mice compared with similar cells from Balb/c mice (Fig. 1A and B) as well as NOR and C57BL/6 mice (Fig. 1C and D). This applied to both activated and resting CD4<sup>+</sup> and CD8<sup>+</sup> Teffs. T-cell activation resulted in marked ganglioside elevation, as previously observed (7).

In addition to GM1 and GD1a, this included two members of the ganglio (GM1) family migrating below GD1a, tentatively identified as GD1b and GT1b, which are converted to GM1 by N'ase treatment of the HPTLC plates. Densitometric quantifications (Table 1) revealed roughly equivalent deficiencies in CD4<sup>+</sup> and CD8<sup>+</sup> Teffs; the GM1/GD1a deficit for 8-week-old NOD Teffs was ~57% for resting and 68% for activated cells compared with Balb/c mice. Similar or even greater GM1 deficiency was noted in NOD Teffs compared with Teffs from NOR and C57BL/6 mice (Fig. 1C and D). Corresponding values for CD4<sup>+</sup> and CD8<sup>+</sup> 11-week-old NOD Teffs compared with Balb/c Teffs were 41 and 71%, respectively.

We performed the remaining comparison studies with NOD versus Balb/c mice, the latter being representative of the three nondiabetic mouse strains we studied in regard to GM1 sufficiency. Cell-surface presentation of gangliosides, determined by flow cytometry, showed similar differences with respect to GM1 (Fig. 2Ba and Ca) and GD1a (Fig. 2Bb

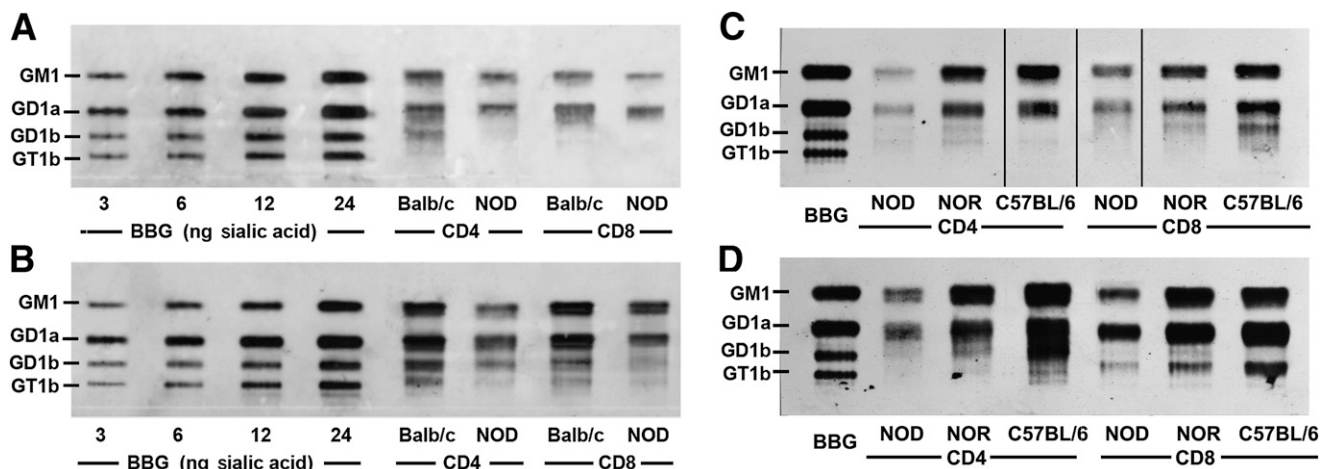


**FIG. 1.** Ganglioside deficiency in NOD Teffs. CD4<sup>+</sup> and CD8<sup>+</sup> Teffs were isolated from spleens of 8-week-old NOD and Balb/c mice and activated with anti-CD3/anti-CD28. Lipid extracts from freshly purified (resting) and activated cells were resolved by HPTLC and GM1 family gangliosides revealed by N<sup>+</sup>ase treatment, followed by CtxB-HRP overlay. **A:** Resting NOD and Balb/c Teffs (20  $\mu$ g protein). **B:** Activated NOD and Balb/c Teffs (10  $\mu$ g protein). **C:** Resting NOD, NOR, and C57BL/6 Teffs (20  $\mu$ g protein). **D:** Activated NOD, NOR, and C57BL/6 Teffs (10  $\mu$ g protein). Bovine brain ganglioside (BBG) mixtures of varying amounts were run simultaneously to provide standard curves for quantification (A and B). Resting and activated NOD Teffs both possessed significantly less GM1 and GD1a than Balb/c, NOR, and C57BL/6 Teffs. Note the significant increases of Teff GM1 upon activation. Densitometry results are given in Table 1. Note that in C, lanes 4 and 5 were cut out from the original TLC blot and switched (as designated by two black lines) in order to preserve the order NOD, NOR, C57BL/6.

and Cb). Qualitative depictions of these deficiencies were obtained with cytochemical staining of activated Teffs for GM1 (Fig. 2Aa) and GD1a (Fig. 2Ab).

**Deficient calcium influx via TRPC5 channels in NOD Teffs.** In view of the critical role of GM1 cross-linking for TRPC5 channel activation (7), we monitored the latter with fura-2 fluorescent Ca<sup>2+</sup> indicator applied to activated Teffs. In contrast to Balb/c-activated Teffs, which demonstrated robust elevation of intracellular Ca<sup>2+</sup> ([Ca<sup>2+</sup>]<sub>i</sub>) in the presence of CtxB or Gal-1, NOD Teffs showed significantly diminished Ca<sup>2+</sup> influx under similar conditions (Fig. 3). Much of this deficiency was corrected by preincubation of the NOD Teffs with GM1-containing solution after activation but

before fura-2 application and testing. Identification of the operative Ca<sup>2+</sup> channel as TRPC5 was supported by effective blockade with SK&F 96365, a TRP channel blocker (17) (Fig. 3A and B). This Ca<sup>2+</sup> channel was strongly upregulated in Teffs during polyclonal activation (7), whereas the pivotal role of GM1 cross-linking in elevating [Ca<sup>2+</sup>]<sub>i</sub> was reflected in the ablation of Ca<sup>2+</sup> influx in Balb/c Teffs by non-cross-linking anti-GM1 Ab (Fig. 3A and B); nonspecific IgG had no effect (Fig. 3B).

**Failure of Treg suppression of NOD Teffs.** To compare the ability of Teffs from NOD and Balb/c mice to experience Treg-mediated growth inhibition, mixtures of varying ratios of activated Teffs and Tregs from the same and alternate

**TABLE 1**  
Ganglioside quantification by densitometry

Variable		n	8 Weeks		n	11 Weeks		
			GM1	GD1a		GM1	GD1a	
Preactivated								
CD4	NOD	11	161 ± 21	246 ± 31	7	187 ± 11	268 ± 31	
	Balb/c	4	540 ± 89*	758 ± 73†	8	482 ± 31‡	757 ± 18*	
	NOR	4	543 ± 61†	553 ± 232*				
	C57BL/6	4	753 ± 70†	693 ± 213*				
CD8	NOD	9	146 ± 13	370 ± 41	7	193 ± 7	245 ± 43	
	Balb/c	4	261 ± 14‡	574 ± 156*	7	261 ± 6‡	448 ± 7†	
	NOR	4	322 ± 68	1,066 ± 189†				
	C57BL/6	4	596 ± 58	957 ± 348*				
Activated								
CD4	NOD	16	287 ± 47	260 ± 24	10	379 ± 58	477 ± 64	
	Balb/c	7	1,309 ± 163†	1,360 ± 166‡	7	1,595 ± 106‡	1,593 ± 118‡	
	NOR	4	1,185 ± 149†	1,477 ± 379*				
	C57BL/6	4	1,775 ± 232†	1,675 ± 690*				
CD8	NOD	13	404 ± 51	603 ± 72	7	321 ± 50	309 ± 74	
	Balb/c	4	996 ± 620‡	1,119 ± 315‡	7	748 ± 60‡	1,593 ± 249†	
	NOR	4	1,235 ± 144†	1,545 ± 160†				
	C57BL/6	4	1,724 ± 256†	1,938 ± 138‡				

Values are shown as mean ± SEM in pmol/mg protein. Gangliosides revealed on the HPTLC plate were quantified by densitometric analysis with a FluorChem Imaging system (Alpha Innotech); bovine brain ganglioside was used as standard. Two-tailed Student *t* test: \**P* < 0.05, †*P* < 0.01, and ‡*P* < 0.001 compared with NOD.

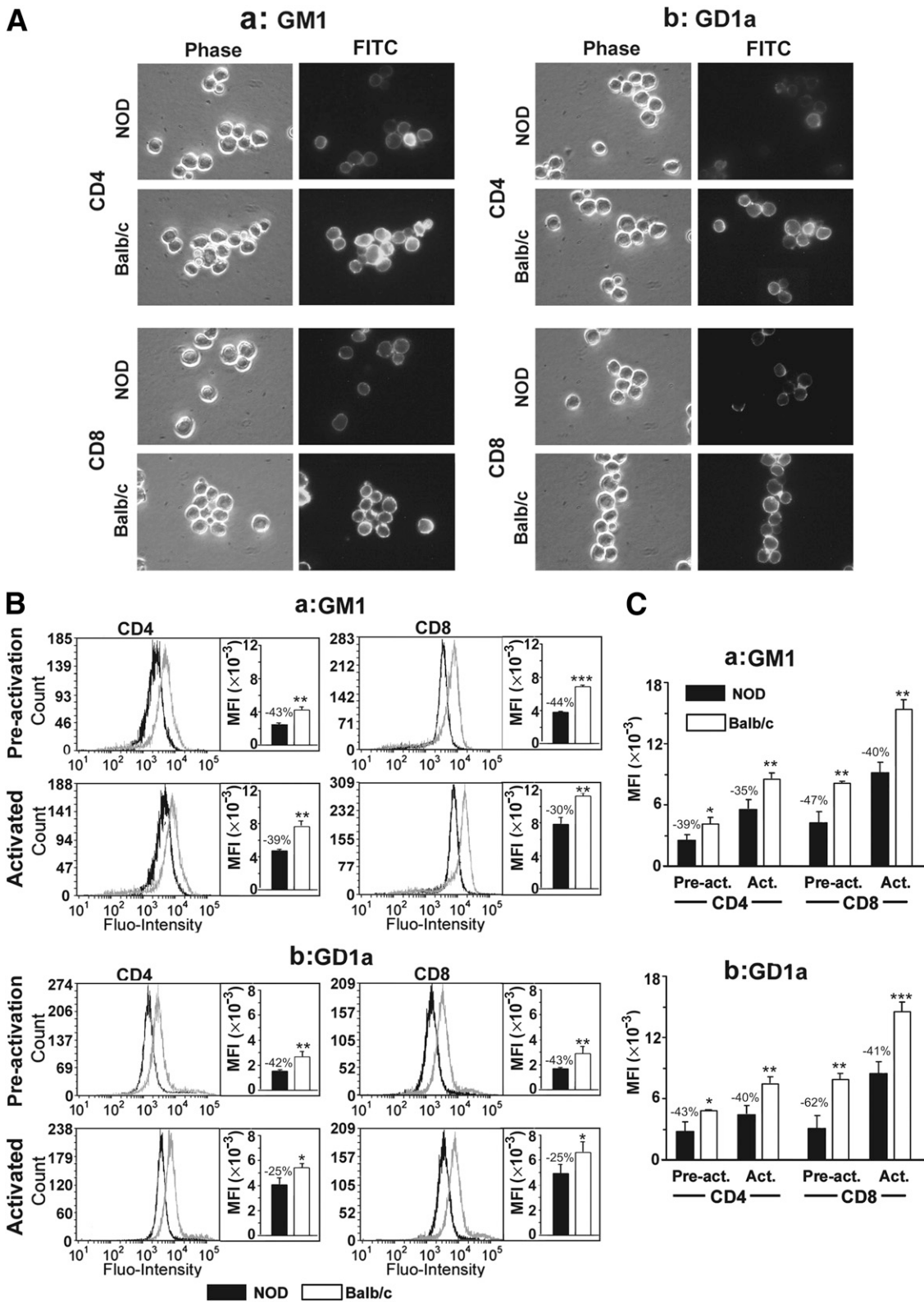
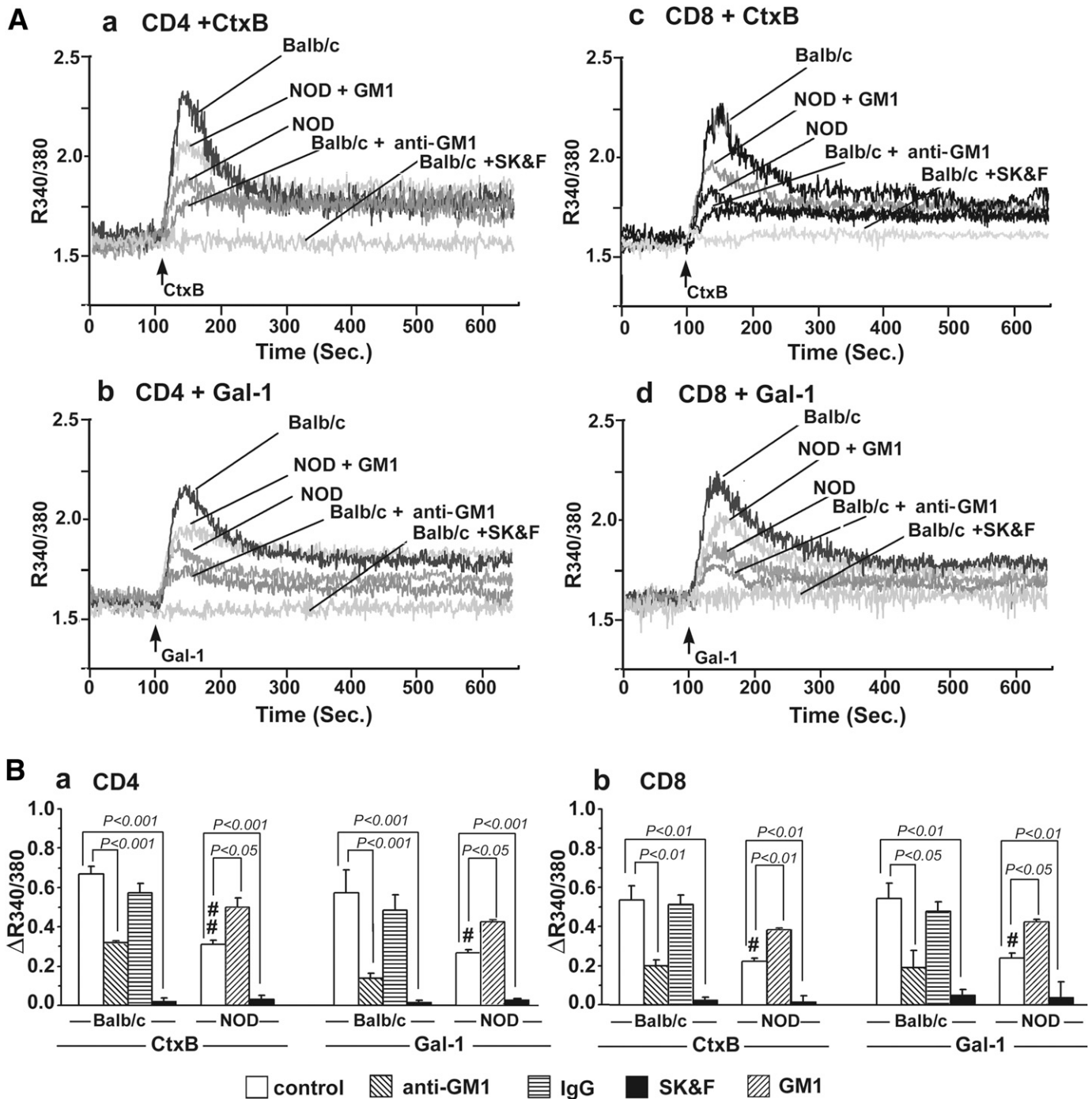


FIG. 2. Reduced GM1 (a) and GD1a (b) on the surface of NOD Teffs. NOD and Balb/c CD4<sup>+</sup> and CD8<sup>+</sup> Teffs, both resting and activated, were separately stained with CtxB-FITC and anti-GD1a mAb plus anti-mouse IgG-FITC. A: Phase contrast and fluorescent photomicrographs are shown of activated Teffs prepared from 8-week-old mice. B: Flow cytometry shows quantitative deficiencies of surface GM1 and GD1a in resting and activated CD4<sup>+</sup> and CD8<sup>+</sup> Teffs from 8-week-old NOD mice. C: Similar analysis is shown of Teffs from 11-week-old mice. Depicted data represent one representative experiment done in triplicate. The error bars show the SEM. Similar results were obtained in 3–4 independent experiments. Two-tailed Student *t* test was used for statistical analysis: \**P* < 0.05, \*\**P* < 0.01, and \*\*\**P* < 0.001. MFI, mean fluorescence intensity.



**FIG. 3.** Reduced  $\text{Ca}^{2+}$  influx in activated NOD Tregs treated with CtxB and Gal-1. Activated cells were pretreated with N'ase and subjected to  $[\text{Ca}^{2+}]_i$  measurement with fura-2 indicator. **A:**  $[\text{Ca}^{2+}]_i$  elevation promoted by CtxB (5  $\mu\text{g}/\text{mL}$ ) or Gal-1 (20  $\mu\text{g}/\text{mL}$ ). Each curve was the average of 3–4 independent runs. **B:** Peak elevation of  $[\text{Ca}^{2+}]_i$ , showing reduced  $\text{Ca}^{2+}$  response in NOD compared with Balb/c Tregs. The role of GM1 was demonstrated by significant recovery of  $\text{Ca}^{2+}$  response in NOD Tregs supplemented with exogenous GM1 and blockade of  $\text{Ca}^{2+}$  response in Balb/c cells pretreated with non-cross-linking anti-GM1 Ab; nonspecific IgG had no effect. Blockade of  $\text{Ca}^{2+}$  response by SK&F 96365 (100  $\mu\text{mol}/\text{L}$ ) indicated involvement of TRP channels, previously demonstrated to be TRPC5 (7). Data are average  $\pm$  SEM (error bars) of 3–4 runs. Two-tailed Student *t* test was used for statistical analysis. #*P* < 0.05; ##*P* < 0.01, NOD compared with Balb/c.

mouse strains were cocultured, and  $[\text{^3H}]\text{TdR}$  incorporation was determined. Cultures exhibiting effective suppression showed rapid decrease of incorporated counts with increasing Tregs between Treg/Teff ratios of 1/0 and 1/1, followed by plateau formation at ratios between 1/1 and 1/4. NOD Tregs showed rather minimal suppression with NOD Tregs compared with Balb/c Tregs in the presence of Balb/c Tregs (Fig. 4A). The results with mixed cultures were more

revealing, in that proliferation of  $\text{CD4}^+$  Tregs from Balb/c mice was largely inhibited by Tregs from both Balb/c and NOD mice, whereas  $\text{CD4}^+$  Tregs from NOD mice were resistant to Treg suppression from both donors (Fig. 4B). Similar results were obtained with  $\text{CD8}^+$  Tregs, although inhibition by Tregs appeared somewhat less effective (Fig. 4A and B). Significantly, Treg-induced growth inhibition was restored in NOD  $\text{CD4}^+$  and  $\text{CD8}^+$  cells by preincubation

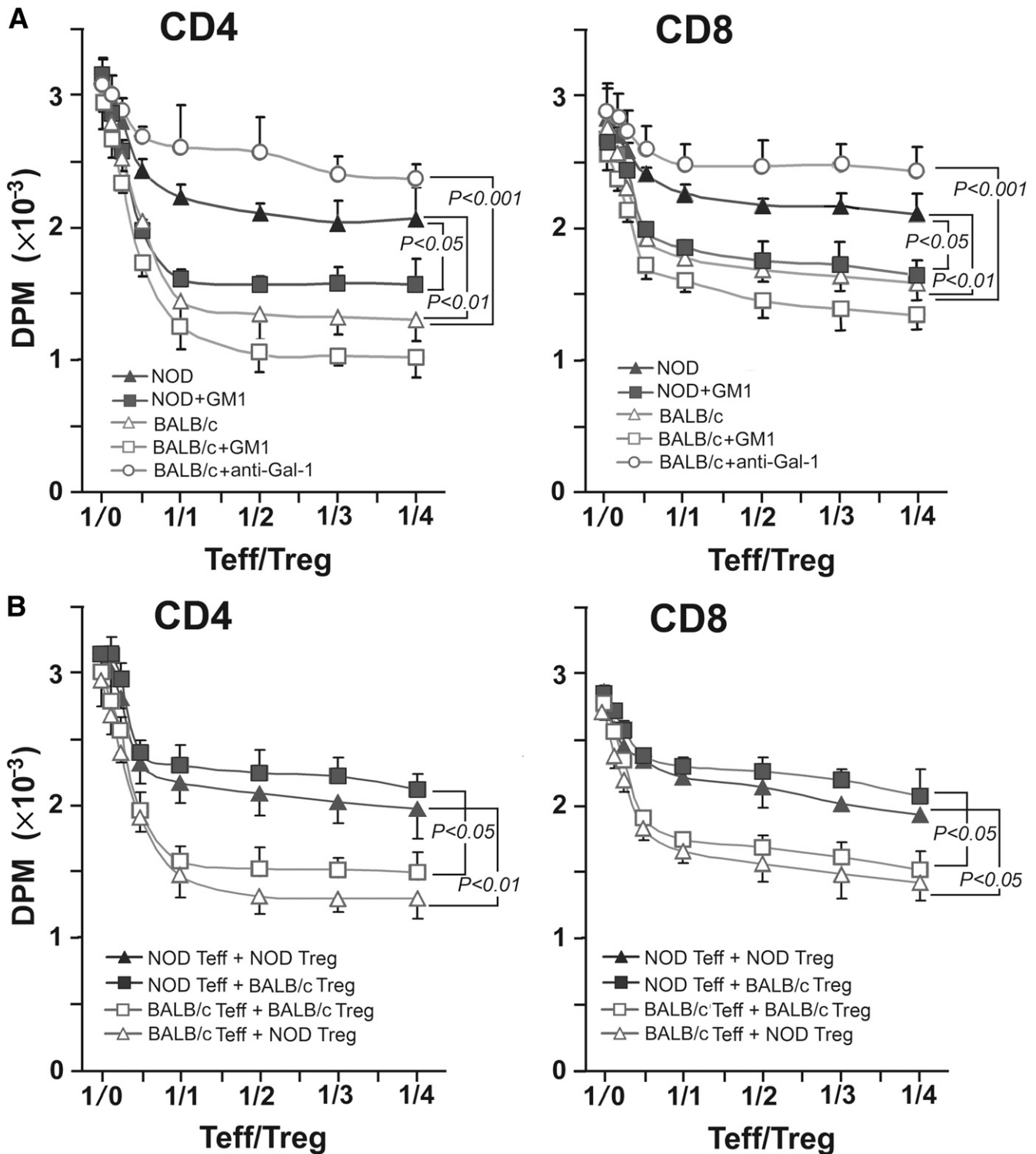


**FIG. 4.** Treg-induced growth inhibition of NOD Teffs mediated by Gal-1/GM1 interaction. Activated CD4<sup>+</sup> and CD8<sup>+</sup> Teffs were assayed for [<sup>3</sup>H]TdR uptake in the presence of variable amounts of Tregs. **A:** Tregs and Teffs from the same mouse showed impaired growth inhibition for NOD compared with Balb/c cells. Reactivity was restored by pretreatment of NOD Teffs with GM1. Anti-Gal-1 Ab abolished growth inhibition of Balb/c Teffs by Balb/c Tregs. **B:** Growth inhibition of activated Teffs by activated Tregs from the same or other strain donors. Background counts were obtained with Treg cultures only and subtracted from mixed culture counts in proportion to the number of Tregs. Responses of NOD Teffs were significantly less for both Tregs than Balb/c Teffs. Statistical analysis: one-way ANOVA with repeated measurements and the Tukey multiple comparison post-test. The error bars show the SEM.

of the activated Teffs with GM1 (Fig. 4A). Such treatment also appeared to marginally enhance suppression of the normally responsive Balb/c Teffs. The latter cells failed to respond to Tregs in the presence of anti-Gal-1 (Fig. 4A), indicating a prominent role for Gal-1 in Teff suppression.

**Failure of Gal-1- and CtxB-induced suppression of NOD Teffs.** Functional deficiency of NOD Teffs was also indicated in their failure to respond to GM1 cross-linking agents. In contrast to concentration-dependent inhibition of [<sup>3</sup>H]TdR incorporation into Balb/c Teffs by Gal-1 and

CtxB, NOD Teffs responded only marginally to both agents with suppressed proliferation (Fig. 5). As documented in Fig. 4, prior incubation with GM1 restored suppression of NOD Teffs and enhanced the already significant suppression of Balb/c Teffs. The latter inhibition could be blocked with non-cross-linking anti-GM1 Ab (Fig. 5B). These studies demonstrated for the first time that GM1 deficiency in NOD Teffs is responsible for their resistance to suppression by Tregs.

## DISCUSSION

Autoimmune destruction of insulin-producing pancreatic  $\beta$ -cells is recognized as the key pathogenic feature of type 1 diabetes in patients and in the NOD mouse model (18). Lack of tolerance in autoimmune conditions has been postulated to at least partly result from failed Treg suppression of antigen-specific Teffs. Although several new classes of Tregs have recently been described, we limited these studies to classical  $CD4^+CD25^+$  Tregs, characterized by expression of FoxP3 (19,20). Several studies exploring possible defects in one or both cell types have produced somewhat conflicting results for the cause of failed suppression.

Quantitative deficiency of Tregs was reported in peripheral blood of type 1 diabetic patients compared with nondiabetic subjects (21), whereas other studies found normal levels of Tregs in type 1 diabetic subjects (22–24) as well as NOD mice (3,25,26). Moreover, Tregs appear to be expressed at increased frequency in children with newly diagnosed type 1 diabetes and in at-risk children with diabetes-associated autoantibodies (27). Alternatively,

qualitative defects in suppressor function of Tregs was proposed as another mechanism for failed suppression in subjects with type 1 diabetes (24) and NOD mice (26), the latter allegedly showing age-based decline in natural Treg cell functional potency. Another study, however, found that diabetes onset in NOD mice was only partially explained by defective Treg activity; whereas adequate protection from disease transfer to severe combined immunodeficiency mice was obtained with Tregs from young but not aged donors, Tregs from diabetic NOD mice still protected from disease transfer by pathogenic Teffs (28). The latter study suggested progressive resistance of diabetogenic Teffs to Treg inhibition as salient factor, overt disease correlating with eventual escape of these pathogenic Teffs from transforming growth factor- $\beta$ -dependent regulation by adaptive Tregs. Similar findings were demonstrated in another study that correlated diabetes onset in NOD mice with decreased suppressive activity of Tregs and enhanced pathogenicity of Teffs (29). Two recent studies with NOD mice (3) and subjects with type 1 diabetes (4) have attributed defective regulation primarily to resistance of responding Teffs rather than malfunctioning Tregs.

The current study also suggests that failed suppression of Teffs in NOD mice contributes importantly to the pathogenesis of this murine form of type 1 diabetes. NOD Teffs responded weakly to Balb/c Tregs compared with robust suppression of Balb/c Teffs by NOD or Balb/c Tregs (Fig. 4B). Further probing into this mechanism revealed that this defect correlated with a drastic reduction in the GM1 content of NOD Teffs, both in relation to cellular content (Fig. 1) and cell-surface expression (Fig. 2).  $CD4^+$  and

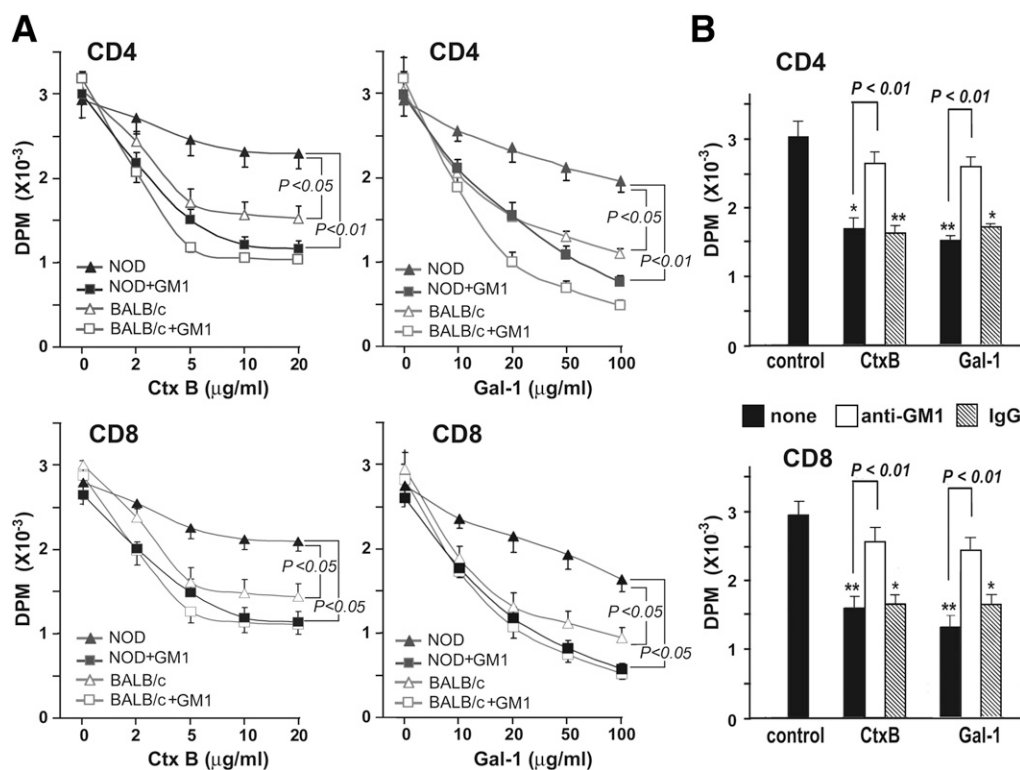


**FIG. 5.** Growth inhibition of Teffs by GM1 cross-linking agents. **A:** Activated  $CD4^+$  and  $CD8^+$  Teffs were assayed for [ $^3H$ ]TdR uptake in the presence of variable amounts of CtxB and Gal-1. Balb/c Teffs showed CtxB and Gal-1 dose-dependent inhibition of cell growth, whereas NOD Teff showed significantly less inhibition to both reagents. NOD Teff inhibition was significantly enhanced by GM1 pretreatment. Statistical analysis: one-way ANOVA with repeated measurements and the Tukey multiple comparison post-test. **B:** Robust response of Balb/c Teffs to CtxB or Gal-1 was blocked by non-cross-linking anti-GM1 IgG, but not by nonspecific IgG. Statistical analysis: two-tailed Student *t* test; \* $P < 0.01$ , \*\* $P < 0.001$  compared with corresponding controls. The error bars show the SEM.

CD8<sup>+</sup> Teffs of NOD mice both expressed significantly less GM1 than Teffs from the other three mouse strains tested (Fig. 1). That GM1 deficiency was the likely cause of failed suppression was suggested by restoration of normal suppression through application of exogenous GM1 to NOD Teffs (Fig. 4A). GM1, similar to gangliosides in general, is able to insert spontaneously into the plasma membrane of cultured cells and subsume normal GM1 functions at that locus (30).

Additional evidence for GM1 involvement in Teff suppression was seen in the failure of Teffs from GM1-deficient mice to be suppressed by normal Tregs (7). Ganglioside GD1a, a N<sup>+</sup>ase-reactive precursor to GM1, showed similar deficiency in NOD Teffs and similar marked elevation during polyclonal activation (Fig. 1). Of note, endogenous N<sup>+</sup>ase is upregulated during T-cell activation (31) and may contribute to the GM1 rise during that process.

Administration of GM1 in vivo to prediabetic NOD mice delayed the onset and reduced the incidence of diabetes (10), providing additional evidence for involvement of this ganglioside in Teff suppression. Previous study of the underlying mechanism demonstrated that cross-linking of GM1 in the Teff plasma membrane triggers a signaling cascade resulting in Ca<sup>2+</sup> influx and immunosuppression (7). This signaling coincides with the above-mentioned activation-triggered elevation of cell surface GM1 observed by us (7) and others (32,33). In this study (Fig. 5) and in a previous report (7), we used CtxB and Gal-1 as GM1 cross-linking ligands, and the interplay of this endogenous lectin with carbohydrate ligand provided a graphic example for turning sugar-encoded information into cellular responses (34). Gal-1 (9) and CtxB (11) both effectively inhibited onset of diabetes in NOD mice and the same was reported for the *Escherichia coli* heat-labile enterotoxin B subunit, a close GM1 cross-linking relative of CtxB (35). Those findings are consonant with the general phenomenon of immune modulation by the cholera-like enterotoxins (36). Cross-linking rather than mere binding of GM1 appears to be critical for Teff suppression because ligation of a non-cross-linking IgG anti-GM1 mAb effectively blocked Teff suppression by CtxB and Gal-1 (Fig. 5B). This proposed role for GM1 (and indirectly GD1a) provides a rationale for its potency in suppressing diabetes in NOD mice (10) and disease onset in other animal models of autoimmunity.

Gal-1 has been proposed as a key effector of Treg-mediated suppression based on its upregulation in such cells after TCR activation and ability to induce suppression of activated Teffs (7,37). It is released from cells by a novel secretory mechanism (38) and can then immediately bind to glycoconjugates on cell surfaces or function as a soluble homodimer, or both. Both Gal-1 populations are strongly upregulated during Treg activation (7). Blockade of Gal-1 binding reduced the inhibitory activity of human and mouse Tregs (37), as also shown here with anti-Gal-1 Ab (Fig. 4A). Further indication of its activity as negative regulator of the immune response is seen in Gal-1 suppression of other autoimmune animal models such as experimental autoimmune encephalitis (7,39,40), collagen-induced arthritis (41), experimental colitis (42), and concanavalin A-induced hepatitis (43).

Similar to other molecular targets for growth regulation, Gal-1 can bind to distinct human cell surface glycoproteins, as demonstrated by its interaction with CD7 and fibronectin receptors (44,45). However, Gal-1 can also bind to cell surface glycolipids when suitably presented (7,46). The importance of microdomain integrity for the highly specific binding of Gal-1 to GM1 in SK-N-MC neuroblastoma cells, whose

GM1 presentation is increased by a surface ganglioside N<sup>+</sup>ase, and the ensuing growth inhibition upon differentiation underscore a functional role of Gal-1/GM1 interaction beyond immune regulation (47,48). Additional evidence for Gal-1 binding to GM1 of Teffs analogous to that of CtxB was provided by similar suppression of autoimmune encephalitis by Gal-1 and CtxB (7). The latter study demonstrated substantially less binding of Gal-1 to GM1-deficient compared with GM1-sufficient Teffs, thus supporting the conclusion that GM1 is the primary receptor for Gal-1 in activated Teffs.

Gal-1 cross-linking of GM1 on the surface of Teffs triggers a signaling cascade that leads to Ca<sup>2+</sup> influx via TRPC5 channels (6), a member of the canonical subfamily belonging to the TRP superfamily of signal transduction-gated ion channels (49). Calcium influx through this pathway was shown to mediate process outgrowth in neuroblastoma cells and primary neurons (6) as well as immunosuppression of spleen-derived Teffs (7). It was noteworthy that Gal-1/CtxB-mediated Ca<sup>2+</sup> influx via TRPC5 channels was significantly attenuated in NOD compared with Balb/c Teffs, a deficiency remedied to a large extent by prior exposure of the Teffs to GM1 (Fig. 3). Moreover, the robust Ca<sup>2+</sup> influx observed in Balb/c Teffs was effectively blocked by non-cross-linking anti-GM1 Ab (Fig. 3B). Interestingly, similar results were also obtained with CD8<sup>+</sup> T cells, which are now seen to resemble CD4<sup>+</sup> Teffs in having a prominent role in NOD pathogenesis (50). Our recent study demonstrated that TRPC5 channels are weakly expressed in resting CD4<sup>+</sup> T cells but strongly upregulated during polyclonal activation (7). In accord with their proposed function, short hairpin RNA knockdown of TRPC5 eliminated the inhibitory effect of CtxB/Gal-1 on Teff proliferation (7).

In summary, we have determined that CD4<sup>+</sup> and CD8<sup>+</sup> Teffs from NOD mice express significantly less GM1 ganglioside than Teffs from Balb/c, NOR, and C57BL/6 mice, such deficiency correlating with reduced Ca<sup>2+</sup> influx and resistance to Treg suppression. We have demonstrated that effective suppression results from cross-linking of GM1 on the surface of Teffs, leading to TRPC5 channel activation and a sufficient level of Ca<sup>2+</sup> influx. Gal-1, a GM1 cross-linking lectin produced by activated Tregs, suppressed Balb/c Teffs but not NOD Teffs, unless the latter were supplemented with exogenous GM1. Such addition also enhanced TRPC5-mediated Ca<sup>2+</sup> influx in NOD Teffs, indicating that a threshold level of Ca<sup>2+</sup> influx via that channel is essential for Teff suppression. These results suggest a novel mechanism by which pathogenic Teffs evade regulatory suppression in the pathogenesis of type 1 diabetes and point to potential new therapeutic approaches for early detection and treatment of this common disease.

#### ACKNOWLEDGMENTS

This study was supported by a grant (RG 3981A) from the National Multiple Sclerosis Society and a grant from the Foundation of Diabetes Research of New Jersey.

No potential conflicts of interest relevant to this article were reported.

G.W. shared in experimental design and planning of experiments, conducted the experiments depicted in Figs. 2–5, and assisted in manuscript preparation. Z.-H.L. carried out HPTLC (Fig. 1) and assisted in the remaining studies. H.-J.G. participated in the experimental design, provided Gal-1 and anti-Gal-1 Ab, and assisted in manuscript preparation. R.W.L. and D.B. jointly developed the underlying

hypotheses and experimental design, supervised the study, evaluated the results, and prepared the manuscript.

## REFERENCES

- Bisikirska BC, Herold KC. Regulatory T cells and type 1 diabetes. *Curr Diab Rep* 2005;5:104–109
- Piccirillo CA, Tritt M, Sgouroudis E, Albanese A, Pyzik M, Hay V. Control of type 1 autoimmune diabetes by naturally occurring CD4<sup>+</sup>CD25<sup>+</sup> regulatory T lymphocytes in neonatal NOD mice. *Ann N Y Acad Sci* 2005;1051:72–87
- D'Alise AM, Auyeung V, Feuerer M, et al. The defect in T-cell regulation in NOD mice is an effect on the T-cell effectors. *Proc Natl Acad Sci USA* 2008; 105:19857–19862
- Schneider A, Rieck M, Sanda S, Pihoker C, Greenbaum C, Buckner JH. The effector T cells of diabetic subjects are resistant to regulation via CD4<sup>+</sup>FOXP3<sup>+</sup> regulatory T cells. *J Immunol* 2008;181:7350–7355
- Ledeer RW, Wu G. Ganglioside function in calcium homeostasis and signaling. *Neurochem Res* 2002;27:637–647
- Wu G, Lu Z-H, Obukhov AG, Nowycky MC, Ledeen RW. Induction of calcium influx through TRPC5 channels by cross-linking of GM1 ganglioside associated with  $\alpha 5\beta 1$  integrin initiates neurite outgrowth. *J Neurosci* 2007; 27:7447–7458
- Wang J, Lu Z-H, Gabius H-J, Rohowsky-Kochan C, Ledeen RW, Wu G. Cross-linking of GM1 ganglioside by galectin-1 mediates regulatory T cell activity involving TRPC5 channel activation: possible role in suppressing experimental autoimmune encephalomyelitis. *J Immunol* 2009;182:4036–4045
- Fishman PH. Role of membrane gangliosides in the binding and action of bacterial toxins. *J Membr Biol* 1982;69:85–97
- Perone MJ, Bertera S, Shufesky WJ, et al. Suppression of autoimmune diabetes by soluble galectin-1. *J Immunol* 2009;182:2641–2653
- Vieira KP, de Almeida e Silva Lima Zollner AR, Malaguti C, Vilella CA, de Lima Zollner R. Ganglioside GM1 effects on the expression of nerve growth factor (NGF), Trk-A receptor, proinflammatory cytokines and on autoimmune diabetes onset in non-obese diabetic (NOD) mice. *Cytokine* 2008;42:92–104
- Sobel DO, Yankelevich B, Goyal D, Nelson D, Mazumder A. The B-subunit of cholera toxin induces immunoregulatory cells and prevents diabetes in the NOD mouse. *Diabetes* 1998;47:186–191
- Wu GS, Ledeen RW. Quantification of gangliotetraose gangliosides with cholera toxin. *Anal Biochem* 1988;173:368–375
- André S, Kaltner H, Furuike T, Nishimura S, Gabius H-J. Persubstituted cyclodextrin-based glycoclusters as inhibitors of protein-carbohydrate recognition using purified plant and mammalian lectins and wild-type and lectin-gene-transfected tumor cells as targets. *Bioconjug Chem* 2004;15: 87–98
- Siebert H-C, André S, Lu SY, et al. Unique conformer selection of human growth-regulatory lectin galectin-1 for ganglioside GM<sub>1</sub> versus bacterial toxins. *Biochemistry* 2003;42:14762–14773
- Kaltner H, Seyrek K, Heck A, Sinowatz F, Gabius H-J. Galectin-1 and galectin-3 in fetal development of bovine respiratory and digestive tracts. Comparison of cell type-specific expression profiles and subcellular localization. *Cell Tissue Res* 2002;307:35–46
- Lohr M, Lensch M, André S, et al. Murine homodimeric adhesion/growth-regulatory galectins-1, -2 and -7: comparative profiling of gene/promoter sequences by database mining, of expression by RT-PCR/immunohistochemistry and of contact sites for carbohydrate ligands by computational chemistry. *Folia Biol (Praha)* 2007;53:109–128
- Minke B, Cook B. TRP channel proteins and signal transduction. *Physiol Rev* 2002;82:429–472
- Atkinson MA, Eisenbarth GS. Type 1 diabetes: new perspectives on disease pathogenesis and treatment. *Lancet* 2001;358:221–229
- Sakaguchi S, Sakaguchi N, Asano M, Itoh M, Toda M. Immunologic self-tolerance maintained by activated T cells expressing IL-2 receptor  $\alpha$ -chains (CD25). Breakdown of a single mechanism of self-tolerance causes various autoimmune diseases. *J Immunol* 1995;155:1151–1164
- Fontenot JD, Rudensky AY. A well adapted regulatory contrivance: regulatory T cell development and the forkhead family transcription factor Foxp3. *Nat Immunol* 2005;6:331–337
- Kukreja A, Cost G, Marker J, et al. Multiple immuno-regulatory defects in type-1 diabetes. *J Clin Invest* 2002;109:131–140
- Brusko T, Wasserfall K, McGrail K, et al. No alterations in the frequency of FOXP3<sup>+</sup> regulatory T-cells in type 1 diabetes. *Diabetes* 2007;56:604–612
- Putnam AL, Vendrame F, Dotta F, Gottlieb PA. CD4<sup>+</sup>CD25<sup>high</sup> regulatory T cells in human autoimmune diabetes. *J Autoimmun* 2005;24:55–62
- Lindley S, Dayan CM, Bishop A, Roep BO, Peakman M, Tree TI. Defective suppressor function in CD4<sup>+</sup>CD25<sup>(+)</sup> T-cells from patients with type 1 diabetes. *Diabetes* 2005;54:92–99
- Mellanby RJ, Thomas D, Phillips JM, Cooke A. Diabetes in non-obese diabetic mice is not associated with quantitative changes in CD4<sup>+</sup> CD25<sup>+</sup> Foxp3<sup>+</sup> regulatory T cells. *Immunology* 2007;121:15–28
- Tritt M, Sgouroudis E, d'Hennezel E, Albanese A, Piccirillo CA. Functional waning of naturally occurring CD4<sup>+</sup> regulatory T-cells contributes to the onset of autoimmune diabetes. *Diabetes* 2008;57:113–123
- Oling V, Marttila J, Knip M, Simell O, Ilonen J. Circulating CD4<sup>+</sup>CD25<sup>high</sup> regulatory T cells and natural killer T cells in children with newly diagnosed type 1 diabetes or with diabetes-associated autoantibodies. *Ann N Y Acad Sci* 2007;1107:363–372
- You S, Belghith M, Cobbold S, et al. Autoimmune diabetes onset results from qualitative rather than quantitative age-dependent changes in pathogenic T-cells. *Diabetes* 2005;54:1415–1422
- Gregori S, Giarratana N, Smiroldo S, Adorini L. Dynamics of pathogenic and suppressor T cells in autoimmune diabetes development. *J Immunol* 2003;171:4040–4047
- Wu G, Ledeen RW. Gangliosides as modulators of neuronal calcium. *Prog Brain Res* 1994;101:101–112
- Wang P, Zhang J, Bian H, et al. Induction of lysosomal and plasma membrane-bound sialidases in human T-cells via T-cell receptor. *Biochem J* 2004;380:425–433
- Brumeanu T-D, Preda-Pais A, Stoica C, Bona C, Casares S. Differential partitioning and trafficking of GM gangliosides and cholesterol-rich lipid rafts in thymic and splenic CD4 T cells. *Mol Immunol* 2007;44:530–540
- Tuosto L, Parolini I, Schröder S, Sargiacomo M, Lanzavecchia A, Viola A. Organization of plasma membrane functional rafts upon T cell activation. *Eur J Immunol* 2001;31:345–349
- Gabius H-J (Ed.). *The Sugar Code. Fundamentals of Glycosciences*. Weinheim, Germany, Wiley-VCH, 2009
- Ola TO, Williams NA. Protection of non-obese diabetic mice from autoimmune diabetes by *Escherichia coli* heat-labile enterotoxin B subunit. *Immunology* 2006;117:262–270
- Salmond RJ, Luross JA, Williams NA. Immune modulation by the cholera-like enterotoxins. *Expert Rev Mol Med* 2002;4:1–16
- Garín MI, Chu CC, Golshayan D, Cernuda-Morollón E, Wait R, Lechler RI. Galectin-1: a key effector of regulation mediated by CD4<sup>+</sup>CD25<sup>+</sup> T cells. *Blood* 2007;109:2058–2065
- Cooper DN, Barondes SH. Evidence for export of a muscle lectin from cytosol to extracellular matrix and for a novel secretory mechanism. *J Cell Biol* 1990;110:1681–1691
- Toscano MA, Bianco GA, Ilarregui JM, et al. Differential glycosylation of T<sub>H</sub>1, T<sub>H</sub>2 and T<sub>H</sub>17 effector cells selectively regulates susceptibility to cell death. *Nat Immunol* 2007;8:825–834
- Offner H, Celnik B, Bringman TS, Casentini-Borocz D, Nedwin GE, Vandenbark AA. Recombinant human  $\beta$ -galactoside binding lectin suppresses clinical and histological signs of experimental autoimmune encephalomyelitis. *J Neuroimmunol* 1990;28:177–184
- Rabinovich GA, Daly G, Dreja H, et al. Recombinant galectin-1 and its genetic delivery suppress collagen-induced arthritis via T cell apoptosis. *J Exp Med* 1999;190:385–398
- Santucci L, Fiorucci S, Rubinstein N, et al. Galectin-1 suppresses experimental colitis in mice. *Gastroenterology* 2003;124:1381–1394
- Santucci L, Fiorucci S, Cammilleri F, Servillo G, Federici B, Morelli A. Galectin-1 exerts immunomodulatory and protective effects on concanavalin A-induced hepatitis in mice. *Hepatology* 2000;31:399–406
- Rappl G, Abken H, Mucche JM, et al. CD4<sup>+</sup>CD7<sup>+</sup> leukemic T cells from patients with Sézary syndrome are protected from galectin-1-triggered T cell death. *Leukemia* 2002;16:840–845
- André S, Sanchez-Ruderisch H, Nakagawa H, et al. Tumor suppressor p16INK4a—modulator of glycomic profile and galectin-1 expression to increase susceptibility to carbohydrate-dependent induction of anoikis in pancreatic carcinoma cells. *FEBS J* 2007;274:3233–3256
- Kopitz J. Glycolipids. In *The Sugar Code. Fundamentals of Glycosciences*. Gabius H-J, Ed. Weinheim, Germany, Wiley-VCH, 2009, p. 177–198
- Kopitz J, von Reitzenstein C, André S, et al. Negative regulation of neuroblastoma cell growth by carbohydrate-dependent surface binding of galectin-1 and functional divergence from galectin-3. *J Biol Chem* 2001; 276:35917–35923
- Kopitz J, von Reitzenstein C, Burchert M, Cantz M, Gabius HJ. Galectin-1 is a major receptor for ganglioside GM<sub>1</sub>, a product of the growth-controlling activity of a cell surface ganglioside sialidase, on human neuroblastoma cells in culture. *J Biol Chem* 1998;273:11205–11211
- Clapham DE, Runnels LW, Strübing C. The TRP ion channel family. *Nat Rev Neurosci* 2001;2:387–396
- Walter U, Santamaria P. CD8<sup>+</sup> T cells in autoimmunity. *Curr Opin Immunol* 2005;17:624–631